Transformation of amorphous TiO₂ to a hydronium oxofluorotitanate and applications as an HF sensor

Leah N. Appelhans*, Patrick S. Finnegan¹, Lee T. Massey¹, Ting S. Luk^{1,2}, Mark A.

Rodriguez¹, Michael T. Brumbach¹, Bonnie McKenzie¹, Julia Craven-Jones¹

¹Sandia National Laboratories, P.O. Box 5800, Albuquerque, NM 87185, USA

²Center for Integrated Nanotechnologies (CINT-SNL), Sandia National Laboratories, P.O.

Box 5800, NM, 87185, USA

* corresponding author: Sandia National Laboratories, PO Box 5800, Mail Stop 0888,

Albuquerque, NM 87185-0888, United States. Tel.: +1 505 844 1737

Abstract

Amorphous titania thin films were examined for use as the active material in a polarimetry based HF sensor. The amorphous titania films were found to be sensitive to vapor phase HF and the reaction product was identified as a hydronium oxofluorotitanate phase, which has previously only been synthesized in aqueous solution. The extent of reaction varied both with vapor phase HF concentration, relative humidity, and the exposure time. HF concentrations as low as 1 ppm could be detected for exposure times of 120 hrs.

Keywords: hydrofluoric acid, titania, oxyfluoride, HF sensor, polarimetry

1 Introduction

Hydrogen fluoride and hydrofluoric acid are used in a wide range of industrial processes including semiconductor fabrication, petroleum refining and chemical synthesis. HF is highly toxic and corrosive. As such, systems to monitor environmental and laboratory concentrations of HF play an important role in maintaining a safe workplace and limiting environmental impact.

Most commercial technologies rely on active technologies using electrochemical, resistive, or spectroscopic methods for continuous or periodic monitoring. Many of these systems are designed for hazard or release sensing rather than long-term continuous monitoring, although some are suited to both applications. There are also a wide variety of gas sampling methods which vary from single use applications, such as colorimetric sensors, to short duration or dosimetric monitoring, with 'off-site' analysis performed after sample collection. Although many different technologies are available there is a need for a robust passive device that could provide longer duration cumulative sensing of HF in challenging environments, where hazards, accessibility, or space limit the use of active devices. Furthermore, the ability to interrogate such a passive device at a standoff distance would provide additional improvement in application scope and ease of use. One sensing method which has the potential to fulfill both these requirements is the development of a polarization tag that undergoes optical polarization changes on exposure to HF. Such a tag could be used in conjunction with a polarimeter that is capable of measuring the optical polarization properties at a standoff distance [1,2].

The optical polarization sensing method relies on a change in the refractive index of the active material, which, when patterned appropriately, causes a variation in the polarization signal of the device. This is in contrast to many other sensing methods, such as resistive sensing, which most often rely on surface adsorption/desorption rather than a bulk chemical reaction. There are advantages and disadvantages to both methods, but a significant advantage to the optical polarization method is that the necessity of a bulk reaction, and the generation of a material with a unique refractive index subsequent to that reaction, reduces the likelihood of numerous cross-sensitivities to other chemical species, a problem that is a challenge in many chemical sensing technologies.

Although TiO₂ has been used as a gas sensor for a wide variety of analytes[3] it is most often used as a resistive sensor in which adsorption/desorption of gaseous analytes on the surface changes the electron density in the conduction band, resulting in a measurable change in resistivity. Porous titania thin films have also been employed in Fabry-Pérot devices for reversible sensing of organic vapors [4] although the devices were also found to be sensitive to water vapor.

The same group employed porous Si in Fabry-Pérot interferometer devices to sense vapor phase HF [5]. In this case they attributed the shift in the Fabry-Pérot fringes to the dissolution, by the HF, of the thin layer of native oxide within the pores (to form gaseous SiF₄) causing a blue shift in the Fabry-Pérot fringes. The devices were also inert to exposure to hydrochloric, sulfuric, and nitric acids. A number of other groups have used the reaction of SiO₂ and HF to develop surface-acoustic wave (SAW) sensors[6] or microcantilever type sensors [7,8] for HF. To the best of our knowledge titania has not previously been used as the sole active material in any type of HF sensing

One report has used a polarimetric interferometer for the detection of aqueous HF [9]. Using a single-mode potassium ion exchanged (PIE) glass waveguide they were able to detect concentrations of >200 ppm HF in aqueous solution with a response rate that was approximately linear with HF concentration. The active mechanism of HF detection relies on changes in the optical signature caused by etching of the PIE waveguide by HF. The lower detection limit in this application was 200 ppm in aqueous solution and it was not tested for vapor phase exposure. In previous work the same group [10] prepared TiO₂ coated PIE waveguides but, to the best of our knowledge, have not examined the composite structures as HF sensors.

This study investigates the use of amorphous TiO₂ as the active phase in an HF responsive optical polarization sensor. This report will focus on the chemistry and characterization of amorphous TiO₂ and its reaction product with vapor-phase HF. Future reports will detail the development, fabrication, and performance of the polarization tag and detection system for HF sensing.

2 Experimental

Nanopowder titania (titanium (IV) oxide, mixture of rutile and anatase, <100nm particle size (BET), 99.5% trace metals basis) was purchased from Sigma-Aldrich.

Amorphous titania films were deposited by evaporative deposition at thickness of ~100 nm, 150 nm, or 250 nm. Titania films were deposited on blank (unpatterned) silicon wafers and on wafers patterned with a periodic structure designed to produce polarization effects. The deposition was carried out on whole 4-inch round Si or SOI wafers in a TRC3460 Temescal E-beam evaporator, with a TiO₂ ingot source installed, and planetary carousel. The chamber was pumped down to ultra-high vacuum 5E⁻⁷ and then O₂ gas was flowed into the chamber through a mass flow controller set at 20%. The chamber reached an approximate steady state pressure of 5.5E⁻⁵. The distance between the source and the wafers was 17.5 inches. A quartz crystal monitor was used to determine the ultimate film thickness of the TiO₂ films. The rate of deposition was calibrated based on profilometer measurements of a witness sample used to calculate a tooling factor used to adjust the quartz monitor crystal feedback, for a real-time deposition rate.

Anatase films were obtained by post-deposition rapid thermal anneal. Experimental parameters and XRD characterization are included in the supplementary information.

2.1 HF exposure

Gas phase HF and humidity exposures were carried out using a KIN-TEK gaseous exposure system modified in-house with humidity control. Samples were exposed under a dynamic flow of HF/H₂O vapor in carrier gas (N₂). The HF concentration and humidity levels of the test chamber effluent were measured to determine exposure conditions. The HF concentration was measured using MSA AUER colorimetric HF detection tubes and an MSA AUER pump sampler. The reported accuracy is ±15% above 10 ppm and ±25% in the 5-10 ppm range. Relative humidity (RH) and HF concentration were measured at the start and end of the exposure period and, for exposures >24 hrs, at intervals during the exposure. RH was measured with a Dickson TH300. The HF-exposed RH probe was regularly compared at ambient RH to a non-HF exposed probe to ensure that the HF exposure was not significantly degrading the performance of the instrument. All exposures were carried out at ambient temperature (~23 °C). CAUTION: HF is highly toxic and corrosive, all exposures were carried out in a fume hood, with exhaust streams routed through neutralizing chambers containing MgSO₄. Proper PPE should be worn at all times when handling HF or HF-exposed samples.

2.2 Ellipsometry

Ellipsometry was performed with a J.A. Woollam IR-VASE, infrared variable angle spectroscopic ellipsometer . All samples were prepared with their back side bead blasted to create a highly roughened scattering surface to prevent specular reflection from the back surface to the detector. Ellipsometry measures change in polarization of the specularly reflected light from a known polarized source. The polarization change is represented by $e^{i\Delta}$ * $tan(\psi)$. With the appropriate model, the index of refraction, thickness and uniformity of the film can be extracted by fitting Δ and ψ at different wavelengths and angles of incidence.

2.3 XRD

A Siemens model D500 θ –2 θ powder diffractometer (Bruker AXS, Inc. Madison, WI) was used for data collection with samples maintained at room temperature (25°C). Copper K α (0.15418 nm) radiation was produced via a sealed-tube X-ray source and a diffracted-beam curved graphite monochromator; a conventional scintillation counter was used as the detector. Fixed 0.3° incident beam and scatter slits were used (goniometer radius = 120 mm), and the instrument power settings were 40 kV and 30 mA. A series of powder diffraction patterns were collected using grazing angles of 0.5°, 1.0°, 1.5° and 2.0° θ . The patterns were collected using the following parameters: 10-80° 2 θ range, step-size of 0.05° 2 θ and a count time of 30 seconds. Lattice parameter refinement was performed using Jade (v9.5) software (Materials Data, Inc. Livermore, CA).

2.4 SEM/EDS

Scanning electron microscopy (SEM) was performed on a Zeiss Supra 55VP field emission gun SEM. Energy dispersive X-ray spectroscopy (EDS) was performed using a Bruker QUAD SDD detector and Bruker Esprit analysis software. Samples were sputter-coated with ~10 nm Au/Pd to reduce charging.

2.5 XPS and Auger

XPS was performed using a Kratos Axis Ultra DLD instrument with base pressures less than $5 \cdot 10^{-9}$ Torr. A monochromatic Al K α (1486.7 eV) source was utilized operating at 300 W. The analysis area was an elliptical area of 300 x 700 microns. Survey spectra were recorded with 160

eV pass energy, 500 meV step sizes, and 100 ms dwell times averaged over 10 scans. High resolution spectra were recorded with 20 eV pass energy, 50 meV step sizes, and 100 ms dwell times averaged over 20 scans. Charge neutralization from a filament above the sample was utilized to limit differential charging effects. Data processing was performed with CasaXPS Version 2.3.15. The binding energy axes of all spectra were adjusted to align the main component of the C 1s peak to 284.6 eV.

Auger spectroscopy was performed with a Physical Electronics 690 Auger spectrometer. Operating pressures were less than $2 \cdot 10^{-9}$ Torr. The instrument utilizes a double-pass cylindrical mirror analyzer. Images and spectra were obtained using a field-emission tip with beam energy of 10 kV at 10 nA. Data was processed using the Physical Electronics Multi-Pack software.

3 Results and Discussion

3.1 Film Characterization and HF Exposure

Amorphous titania films were deposited by evaporative deposition at thickness of ~100 nm, 150 nm, or 250 nm. Grazing Incidence X-ray Diffraction (GIXRD) of the films confirmed the amorphous nature. The atomic compositions of the amorphous deposited films were determined by XPS and the O:Ti ratio was found to be 1.9 for each of three samples. A control sample of single crystal rutile titania analyzed by the same methods was found to have an O:Ti ratio of 2.0, as expected, indicating that the amorphous evaporatively deposited films are slightly oxygen deficient. Anatase titania films were also prepared by annealing the amorphous films. The anatase structure of the films was confirmed by GIXRD, and XPS analysis found an O:Ti ratio of 2.0 for films annealed in air at 1050 °C. For XPS and XRD for all TiO₂ films see the Supplementary Information.

The as-deposited amorphous TiO₂ and anatase TiO₂ films were exposed to vapor-phase HF at varying concentrations and relative humidity levels. Exposure of anatase films did not result in any bulk reaction detectable by SEM or XRD but XPS analysis revealed fluorination of the surface. Exposure of amorphous titania films to vapor-phase HF resulted in bulk reaction of the TiO₂ thin film and significant morphological changes to the sample (Figure 1) which varied depending on HF concentration, humidity, and duration.

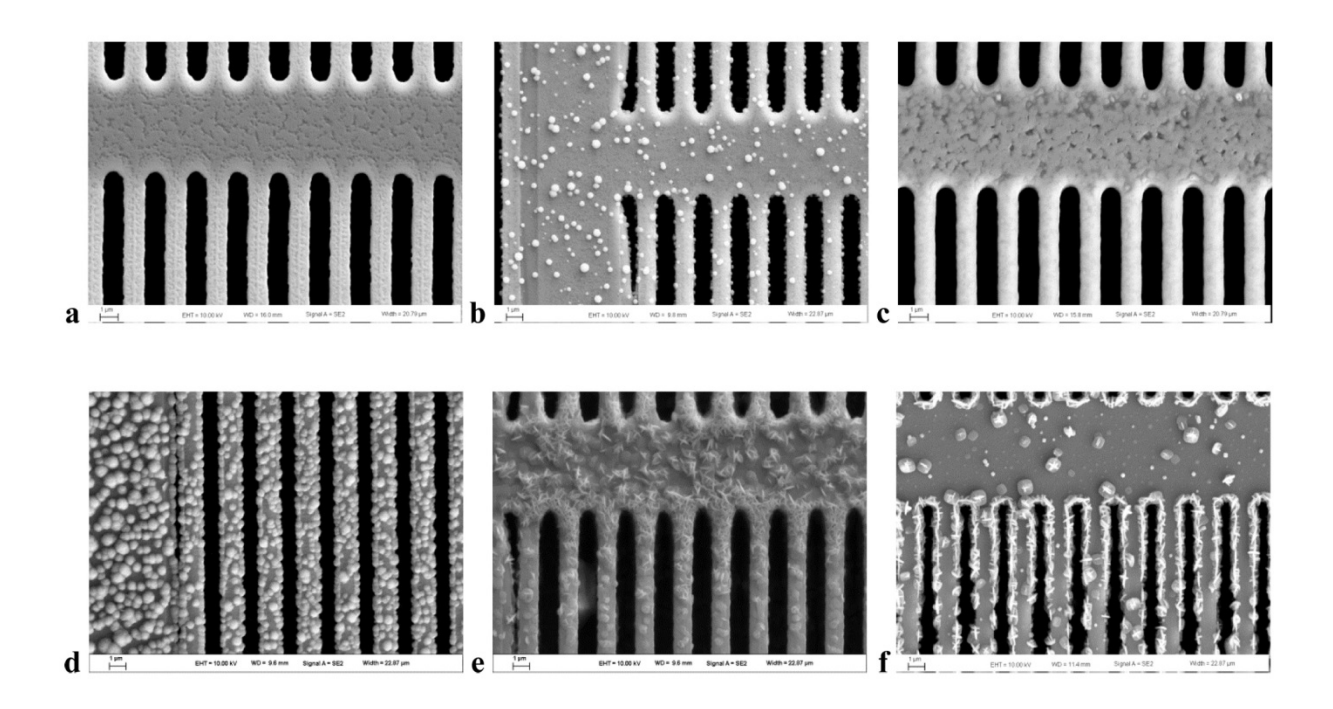


Figure 1: a) Unexposed sample, patterned wafer, TiO₂ coated b) exposed at 20 ppm, 24 hrs, 20%RH c) exposed at 30 ppm, 24 hrs, 20%RH d) exposed at 10 ppm, 96 hrs, 37%RH e) exposed at 20 ppm, 35% RH, 24 hrs f) exposed at 20 ppm, 36% RH, 24 hrs

3.2 Reaction Product Characterization

Grazing incidence X-ray diffraction identified the reaction product formed by the HF-exposure of amorphous titania films as a hydronium oxofluorotitanate phase $(H_3O)_xTiO_yF_2$. The phase has been previously described in the literature by Estruga, et. al. [11].

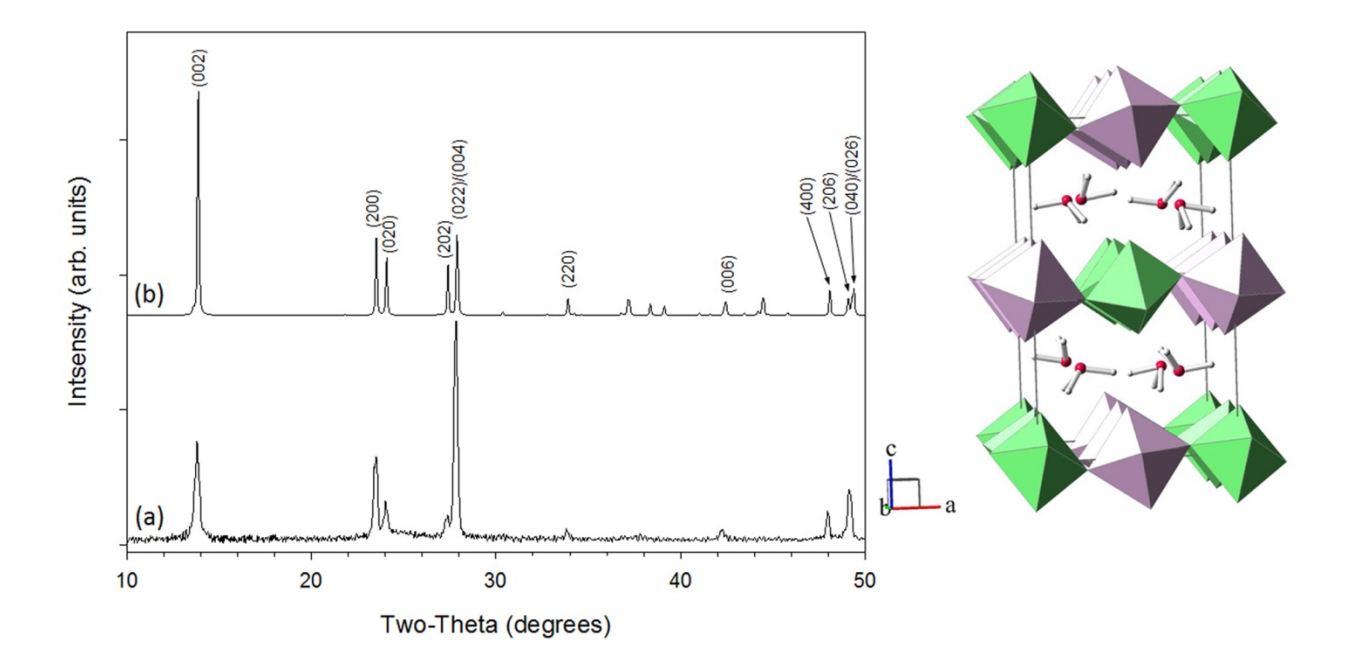


Figure 2: Grazing incidence diffraction pattern and unit cell for the product phase. The observed grazing incidence diffraction pattern (a) as well as the simulated pattern (b) obtained from the structure of $(H_3O)_{2/3}TiO_{4/3}F_2$ (after Estruga, et al. [11]). The (hkl) assignments for the strongest peaks are labeled on the simulated pattern. The unit cell for hydronium oxofluorotitanate phase illustrating $Ti(O,F)_6$ octahedra which form into layers along the a-b plane of the structure with hydronium molecules (red spheres = oxygen atoms) stacking in the c-axis direction between the sheets generated by the $Ti(O,F)_6$ polyhedra. The two colors of polyhedra shown designate the two crystallographically independent Ti atoms (Ti1 Green, Ti2 purple).

In the literature report the hydronium phase was synthesized by thermal decomposition at 85 °C of hexafluorotitanic acid in an aqueous solution of boric acid and HF, and was determined to have the composition (H₃O)_{2/3}TiO_{4/3}F₂. In the absence of boric acid as a fluoride scavenger TiOF₂ was formed. The hydronium oxofluorotitanate structure consists of layers of Ti-O/F octahedra with hydronium ions occupying the interlayers, isostructural to the ammonium oxofluorotitanate phase, NH₄TiOF₃ [12] which is synthesized by the pyrohydrolysis of (NH₄)₂TiF₆ or (NH₄)₂TiOF₄ at 300 °C in steam. Ayllon et. al. found that ammonium could be exchanged into the interlayer of the hydronium phase by treatment in aqueous ammonium solution or with gaseous ammonia.

In this work the hydronium phase was formed via a vapor-phase reaction. It appears that surface-mediated control of reactant stoichiometry at the gas-solid interface as well as the low reaction temperature may favor the formation of the hydronium phase over other oxofluorotitanate phases, such as TiOF₂. Prior work in the literature has demonstrated the importance of vapor-phase versus solution-phase reaction conditions in controlling reaction kinetics and therefore product formation and phase. For example, using a vapor-phase hydrothermal synthesis Liu *et. al.* were able to synthesize anatase TiO₂ nanocrystals with >98% exposed 001} facets [13] from Ti foils. In contrast, reaction under standard liquid-phase hydrothermal conditions in the presence of HF yielded anatase titania with a lower percentage of 001} exposed facets [14,15] although still a significantly higher percentage than by other methods.

Interestingly, in the vapor-phase hydrothermal synthesis Liu *et. al.* [13] report the formation of an intermediate phase forming in the reaction of Ti foil with HF under hydrothermal conditions. The intermediate phase, which formed in the first hour or two of reaction, was identified as

HTiOF₃, and was also reported as being similar in structure to the ammonium oxofluorotitanate phase, consisting of layers of corner-sharing Ti-O/F octahedra. However, the authors propose, based on comparison of the XRD pattern with calculated patterns from optimized structures predicted by DFT calculations, that the interlayer of this phase consists solely of H⁺ rather than hydronium ions. Given that the synthesis temperature is much higher (230 °C) the formation of an analogous dehydrated phase is plausible. However, the calculated structure and XRD pattern of the proposed protic phase are quite similar to that of the hydronium phase fully characterized by Estruga et. al., and may in fact be the same phase. In our case, due to the low reaction temperature and good agreement of the XRD pattern and refined lattice parameters with the hydronium phase, we are confident that product formed is the (H₃O)_xTiO_yF₂ phase.

Refinement of the lattice parameters for the phase reported in this work found a slight expansion relative to the structure reported in the literature for (H₃O)_{2/3}TiO_{4/3}F₂ (see SI), particularly along the c-axis. In the literature characterization of the ammonium analog, NH₄TiOF₃ the authors report [12] the formation of two non-stoichiometric compositions. In both compositions that are sub-stoichiometric in ammonium, (NH₄)_{0.8}TiOF_{2.8} and (NH₄)_{0.3}TiO_{1.1}F_{2.1}, the c-axis is expanded relative to NH₄TiOF₃. If the behavior of the hydronium phase is analogous to the ammonium phase, as might be suggested by the similarity of structure, the expansion in the c-axis suggests that the product formed in this work is slightly more hydronium deficient than the (H₃O)_{2/3}TiO_{4/3}F₂ phase reported in the literature. This result is not surprising given that the literature phase is synthesized in aqueous solution, whereas in this work the reaction takes place in an environment of low-to-moderate relative humidity.

Formation of the hydronium titanium oxyfluoride phase from the amorphous titania thin films begins with the formation of small islands of reaction product on the surface of the titania.

Greater HF concentration or longer duration of exposure leads to both vertical and horizontal growth of the product phase crystallites eventually leading to coalescence and formation of a semi-continuous film under some conditions (Figure 1). The product phase morphology varied widely, especially when the relative humidity during exposure was greater than ~30% (see Figure S22. The GI-XRD patterns of samples with different morphologies all match the hydronium titanium oxyfluoride phase, however, because of the thinness of the product layer, it was not possible to obtain sufficiently high quality patterns for all morphologies to determine if the different morphologies may correspond to small changes in lattice parameters, and possibly stoichiometry, or are simply polymorphic variants of the parent phase.

Scanning electron microscopy (SEM) and atomic force microscopy (AFM) characterization of exposed samples with islanded product formation showed vertical growth up to \sim 500 nm and crystallite diameters of greater than 1 μ m (see Supp. Info. Figures S15, S18, S19). The thickness of the original amorphous TiO₂ films for these samples was 150nm.

Auger spectroscopy analysis of an exposed islanded sample found fluorine present in both the islands and in the interstitial areas. In the interstitial areas the fluorine was localized in a thin surface layer, which could be removed by 15 seconds of sputtering. In contrast, in the product islands or crystallites fluorine was present throughout the thickness of the material, as evidenced by the continued detection of fluorine after both 15 seconds and 2.5 minutes of sputtering. In addition EDS analysis of islanded samples showed a high correlation between increased concentrations of fluorine and the island/crystallite features (see SI).

X-ray photoelectron spectroscopy (XPS) was used to investigate the elemental composition at the surface of both HF exposed anatase and amorphous samples. Ti, O, and adventitious C are found in all samples as expected. In the exposed anatase sample (30 ppm HF, 20%RH, 24 hrs) the F 1s peak is quite weak and occurs at 684 eV. A second weak peak at 688 eV may be present but is difficult to distinguish from the background. In the amorphous exposed sample (10 ppm HF, 37%RH, 24 hrs) the F 1s peaks occur at approximately the same positions (685 eV, major; 688 eV, minor) but are much more intense. XPS spectra are included in the Supplementary Information. In previous literature reports studying the surface fluorination or F-doping of titania the same pair of peaks have been observed. In the work of Yu et. al., in which F-doped titania xerogels are synthesized by reaction of titanium isopropoxide in aqueous solutions in the presence of ammonium fluoride, followed by calcination at 400 °C and above, the peak at 688 eV is the major peak and the peak at 685 eV is the minor peak [16]. The authors ascribe the peak at 688 eV to fluorine in solid solution $TiO_{2-x}F_x$ and the peak at 685 eV to physically adsorbed F. In another study [17] on the surface fluorination of rutile TiO₂ single crystals by exposure to "100% HF steam" at 200 °C, the only observable fluorine peak, which was very weak, was found at 688 eV, leading the authors to conclude that the F was substituted in the lattice, not physically adsorbed, by reference to Yu's previous work. However, in a third study describing the synthesis of N- and F-doped titania [18] the authors synthesized pure TiOF₂ by reaction of TiO₂ with aqueous HF. The pure TiOF₂ exhibited a single F 1s peak at 685 eV. After calcining above 200 °C, the TiOF₂ began to convert to anatase TiO₂ and a second peak at 688 eV was observed. This new peak at 688 eV was attributed to F substitution into the TiO₂ lattice, in agreement with Yu's results. These prior results suggest that the 685 eV peak observed in this study is due to the F in the (H₃O)_xTiO_yF₂ phase and not to surface adsorbed F. The Ti-O/F bonding in the hydronium and TiOF₂ phases is quite similar [11,19], therefore the similarity in F 1s binding energies between the two phases is reasonable. The second F 1s peak at 688 eV is likely

indicative of a small amount of F-doped TiO_2 which could form as an intermediate phase in the transformation of TiO_2 to $(H_3O)_xTiO_vF_2$ under these reaction conditions.

The samples were also analyzed by ellipsometry before and after exposure, as shown in Figure 3 and Figures S15-S17. The refractive index functions derived from the ellipsometry fit show that the refractive index of the exposed film in the $1250 - 5000 \text{ cm}^{-1}$ region ($\lambda = 2.0 - 8.0 \mu m$) is reduced significantly after exposure. In the spectral region of $250-1000 \text{ cm}^{-1}$ ($\lambda = 10 - 40 \mu m$), the absorption (imaginary part of the index of refraction) is also reduced significantly; suggesting that the absorbing material is removed or replaced with low loss material. A simple ungraded fit (assuming a uniform and isotropic morphology) matched well for exposed samples where the reaction product formed a relatively uniform and coherent layer (e.g. Figure 1c). For samples with islanding a more refined modeling approach utilizing a graded Bruggeman uniaxial model [20] provided improved fits (see Figure S20).

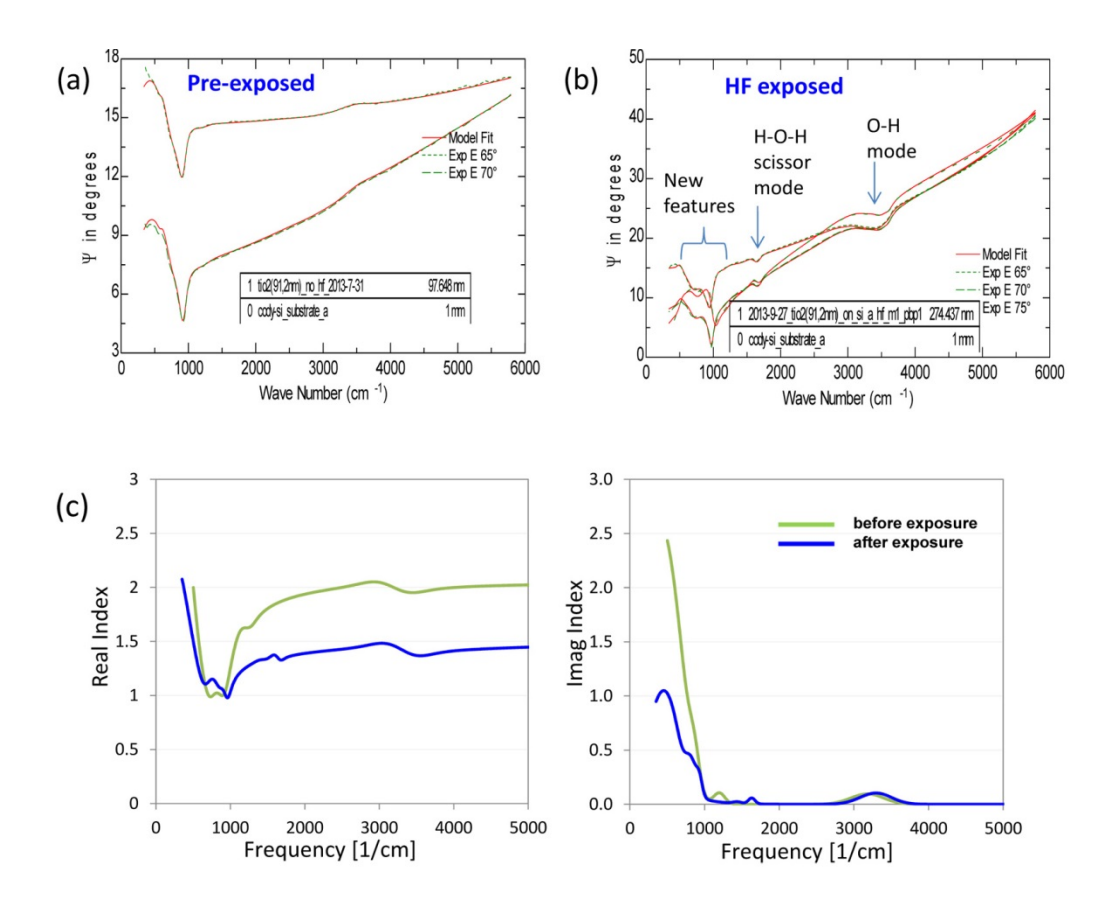


Figure 3: Raw (green) and fitted (red) ellipsometry data for unexposed (a) and HF exposed (b) TiO₂ films. The refractive index functions (c) in the 250-5000 cm⁻¹ region derived from the ellipsometry fits.

Exposures of anatase titania films to vapor-phase HF under identical exposure conditions were also performed. Although surface fluorination was detected by XPS analysis no bulk reaction detectable by SEM or XRD was evident after exposure under these low temperature conditions. In addition, bulk samples of nanoparticulate (avg. particle size <100nm) mixed phase anatase/rutile TiO₂ were also exposed under relatively high HF concentration/high humidity conditions (20-30 ppm, RH>45%) but yielded no detectable formation of the hydronium titanium oxyfluoride phase. These results suggest that the amorphous nature of the deposited TiO₂ films is vital to the observed low-temperature reactivity. This could be due to intrinsic differences in

reactivity/stability between the amorphous and crystalline phases, related to surface morphology and crystalline growth or to differences in accessible surface area, which may be decreased by densification during the amorphous to anatase transformation. Further study using high surface area morphologies of crystalline titania phases [21] would be valuable to elucidate the origins of the observed differences in reactivity.

Finally, bulk exposure of mixed phase TiO₂ nanopowder in the enclosed headspace of a 5wt% aqueous HF solution, at room temperature, yielded gelatinous, amorphous solids, which were not characterized further. Evidently, the high HF concentration and high relative humidity in the enclosed exposure chamber, estimated to be approximately ~150 ppm HF and >97% RH respectively [22], disfavor formation of a crystalline product phase. When amorphous titania thin films were exposed under identical conditions the films were destroyed completely, leaving droplet shaped areas of clear solid residue behind, which was not characterized further.

3.3 Effects of Exposure Conditions on Reactivity

Exposures of amorphous titania films to HF were performed at varying relative humidities and HF concentrations. The extent of reaction during HF exposure was found to depend on a complex interplay between the HF concentration, the humidity during exposure, and the duration of exposure.

The reactivity of amorphous titania films to HF was highly dependent on the relative humidity during the exposures, as might be expected given the composition of the product phase. Samples exposed under dry or low humidity conditions (below ~10%RH) did not undergo reaction even at relatively high concentrations of HF. For example, samples exposed at 30 ppm, 10% relative

humidity, over 96 hours (Figure S24a) did not show any significant changes in post-exposure SEM images, nor was reaction product detected by XRD. In comparison, films exposed for 96 hours to a much lower concentration, but at higher humidity (7 ppm, 30%RH, 96 hours) did show evidence of significant reactivity in the SEM micrographs (Figure S24b). Exposure at high concentration and higher humidity resulted in conversion of the titania to the hydronium oxofluorotitanate reaction product over nearly the entire surface of the polarization tag (see for example Figure 1c, Figure S17, or Figure S23c).

As expected, the reactivity was also highly dependent on the HF concentration. The lowest concentration of HF that resulted in measurable reaction was 1 ppm, at 40%RH, over 120 hours. The sample shows (Figure 4) clear formation of the product phase as was confirmed by XRD. The important role of humidity in facilitating the reaction of amorphous titania with HF is again highlighted by the differing results of exposures at 1 ppm at different humidities. While the sample in Figure 4, exposed at 40% RH for 5 days clearly reacted, an exposure at 1 ppm, 20% RH, for 30 days did not result in any measurable reaction despite the much longer exposure time.

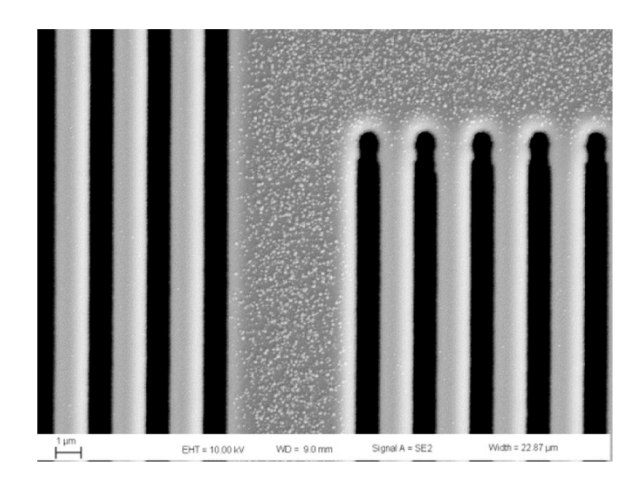


Figure 4: a) Exposure at 1 ppm, 40%RH, 5 days. Formation of the reaction product is clearly evident in the SEM micrographs.

As expected, the extent of reaction also depends on exposure duration. As shown in Figure 5 exposures of different durations at the same concentration and humidity show an increase in the extent of reaction with increased exposure duration.

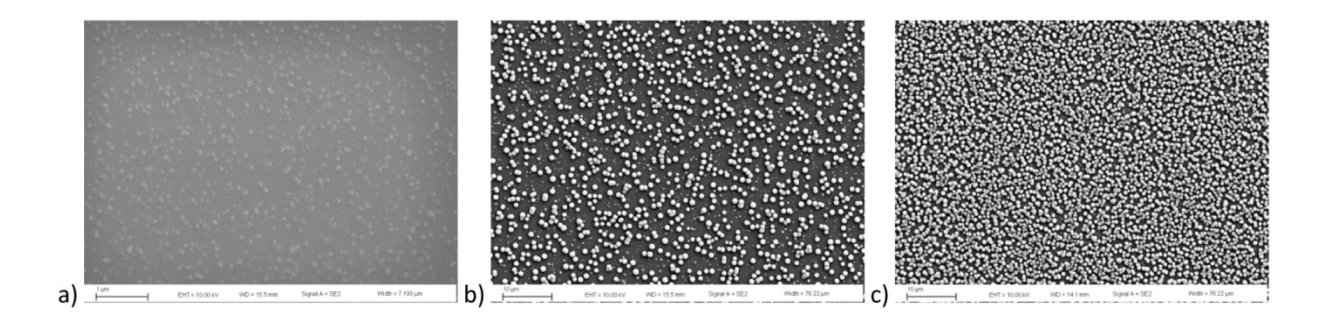


Figure 5. Blanks exposed to 20 ppm HF at ~20%RH for (a) 6hrs (b) 24hrs and (c) 72 hrs. Note that magnification of (a) is greater to allow visualization of the very small areas of reaction.

Defining the total HF dose (ppm.hrs) to be the product of HF concentration (ppm) multiplied by exposure duration (hours) it is clear from Figure 5that the extent of reaction is dose dependent. However, although the extent of reaction increases consistently with increasing dose for

exposures *under the same conditions* (concentration/humidity), comparison of identical doses applied with differing conditions, particularly relative humidity shows that the extent of reaction is not solely dependent on the total accumulated dose (see Figure S23).

The selectivity of amorphous titania to other acid vapors was examined by exposure of amorphous titania films to nitric, hydrochloric, and sulfuric acid (see Supplementary Information for experimental details and characterization). Exposure to ethanol vapor was also tested. These exposures were carried out in an open chamber over a bath of concentrated acid or absolute ethanol without, however, any additional control of relative humidity or vapor phase concentration. Although imprecise, the exposures were performed to determine if measurable changes were produced after exposure to other common laboratory chemicals. No detectable changes in either ellipsometric measurements, SEM examination, or XRD were caused by exposure to any of these chemicals. Exposures to high humidity alone, in a controlled humidity chamber (30 °C, 70%RH, 24 hrs), were also not found to have any effect, as measurable by SEM, XRD, or ellipsometry.

Based on the structural similarity to ammonium oxofluorotitanate phases and literature precedent [11,12] there is a high likelihood that the hydronium oxofluorotitanate phase and, possibly, the amorphous titania precursor films could both be sensitive to exposure to ammonia vapor, particularly in moderate or high humidity conditions. Estruga et. al. [11] reported that simple exposure of hydronium oxofluorotitanate to ammonia/ammonium either in the vaporphase or in solution resulted in incorporation of ammonium cation. Chen *et al.* [23] have used RF sputtered TiO₂ coated optical wave guide sensors with a bromothymol blue sensing layer for the reversible detection of ammonia. This provides some evidence that TiO₂ films may be inert

to ammonia exposure. However, the morphology of the TiO₂ film was not reported in this case, and the exposures were carried out under an dry nitrogen atmosphere. Therefore, for the amorphous films used in our study, and under conditions of higher RH there may still be sensitivity to ammonia. As ammonia is common both in the environment and in laboratory and industrial settings, additional study of the sensitivity to ammonia exposure of both the precursor amorphous titania films and the product phase will be necessary.

4 Conclusions

In this paper the effects of 1-30 ppm vapor-phase HF exposure on amorphous TiO_2 thin films were examined. We have demonstrated the formation of a hydronium oxofluorotitanate phase $(H_3O)_xTiO_yF_2$ from the reaction of vapor phase HF with amorphous TiO_2 thin films. The product morphology and extent of reaction were found to be sensitive to both HF concentration and the relative humidity during exposure. At moderate relative humidity (40%RH) HF concentrations as low as 1 ppm could be detected over relatively short exposure times (5 days). Ellipsometric characterization showed that measurable changes in the complex refractive index of the material could be observed after exposure to HF. Using appropriate sensor patterning and measurement conditions an optical polarization tag can be designed for HF monitoring, with amorphous titania as the active component. Work on the development and evaluation of such an optical polarization tag is ongoing and will be reported in future publications. The results reported here also suggest that, by replacing silica or crystalline titania films with amorphous titania in other HF sensor technologies, such as SAW, microcantilever, or Fabry-Pérot devices, a significant improvement in sensitivity might be realized.

Acknowledgements

This work was funded by the US Department of Energy National Nuclear Security Administration, Office of Defense Nuclear Nonproliferation Research and Development, Dr. Victoria Franques Program Manager.

Sandia National Laboratories is a multi-program laboratory managed and operated by Sandia Corporation, a wholly owned subsidiary of Lockheed Martin Corporation, for the U.S. Department of Energy's National Nuclear Security Administration under contract DE-AC04-94AL85000.

References

- (1) Boye, R. R.; Washburn, C. M.; Scrymgeour, D. A.; Hance, B. G.; Dirk, S. M.; Wheeler, D. R.; Yelton, W. G.; Lambert, T. N. *Advanced Environmental, Chemical, and Biological Sensing Technologies VIII* **2011**, 8024.
- (2) Washburn, C. M.; Jones, J. C.; Vigil, S. R.; Finnegan, P. S.; Boye, R. R.; Hunker, J. D.; Scrymgeour, D. A.; Dirk, S. M.; Hance, B. G.; Strong, J. M.; Massey, L. M.; Brumbach, M. T. *Advanced Fabrication Technologies for Micro/Nano Optics and Photonics VI* **2013**, 8613.
 - (3) Chen, X.; Mao, S. S. Chemical Reviews **2007**, 107, 2891.
- (4) Liang, F.; Kelly, T. L.; Luo, L.-b.; Li, H.; Sailor, M. J.; Li, Y. Y. ACS Applied Materials & Interfaces 2012, 4, 4177.
 - (5) Letant, S. E.; Sailor, M. J. Advanced Materials **2000**, *12*, 355.
- (6) Meulendyk, B. J.; Wheeler, M. C.; da Cunha, M. P. *IEEE Sensors Journal* **2011**, 11, 1768.
- (7) Mertens, J.; Finot, E.; Nadal, M. H.; Eyraud, V.; Heintz, O.; Bourillot, E. *Sensors and Actuators B-Chemical* **2004**, *99*, 58.
- (8) Tang, Y. J.; Fang, J.; Xu, X. H.; Ji, H. F.; Brown, G. M.; Thundat, T. *Analytical Chemistry* **2004**, *76*, 2478.
 - (9) Qi, Z. M.; Matsuda, N.; Itoh, K.; Murabayashi, M. Chemistry Letters 2001, 662.
- (10) Xiao-Min, C.; De-Kui, Q.; Kiminori, I.; Murabayashi, M. *Optical Review* **1996**, *3*, 351.
- (11) Estruga, M.; Casas-Cabanas, M.; Gutierrez-Tauste, D.; Domingo, C.; Ayllon, J. A. *Materials Chemistry and Physics* **2010**, *124*, 904.
- (12) Laptash, N. M.; Maslennikova, I. G.; Kaidalova, T. A. *Journal of Fluorine Chemistry* **1999**, *99*, 133.
- (13) Liu, P.; Wang, Y.; Zhang, H.; An, T.; Yang, H.; Tang, Z.; Cai, W.; Zhao, H. *Small* **2012**, *8*, 3664.

- (14) Yang, H. G.; Sun, C. H.; Qiao, S. Z.; Zou, J.; Liu, G.; Smith, S. C.; Cheng, H. M.; Lu, G. Q. *Nature* **2008**, *453*, 638.
- (15) Zhang, H. M.; Wang, Y.; Liu, P. R.; Han, Y. H.; Yao, X. D.; Zou, J.; Cheng, H. M.; Zhao, H. J. *ACS Applied Materials & Interfaces* **2011**, *3*, 2472.
- (16) Yu, J. C.; Yu, J. G.; Ho, W. K.; Jiang, Z. T.; Zhang, L. Z. *Chemistry of Materials* **2002**, *14*, 3808.
 - (17) Tang, J.; Quan, H.; Ye, J. Chemistry of Materials 2007, 19, 116.
- (18) Li, D.; Ohashi, N.; Hishita, S.; Kolodiazhnyi, T.; Haneda, H. *Journal of Solid State Chemistry* **2005**, *178*, 3293.
 - (19) Vorres, K.; Donohue, J. Acta Crystallographica 1955, 8, 25.
- (20) Cai, W.; Shalaev, V. Optical Metamaterials Fundamentals and applications; Springer, 2010.
- (21) Varghese, O. K.; Gong, D. W.; Paulose, M.; Ong, K. G.; Grimes, C. A. Sensors and Actuators B-Chemical 2003, 93, 338.
- (22) Brosheer, J. C.; Lenfesty, F. A.; Elmore, K. L. *Industrial and Engineering Chemistry* **1947**, *39*, 423.
- (23) Yimit, A.; Itoh, K.; Murabayashi, M. Sensors and Actuators B-Chemical 2003, 88, 239.

Biographies

Leah Appelhans received her Ph.D. degree in Chemistry from Yale University, followed by postdoctoral research at the University of California, Santa Barbara. She joined Sandia National Laboratories in 2009.

Patrick Finnegan is a process engineering and thin film vapor deposition specialist in the Micro-fabrication Facility at Sandia National Laboratories.

Lee Massey is a laboratory technologist at Sandia National Laboratories with a B.S. in Chemical Engineering. He works primarily in the areas of adhesive bonding and encapsulation.

Ting S. Luk received his Ph.D. from the State University of New York at Stony Brook, in 1981. He joined Sandia National Laboratories in 1999 and studied nonlinear optical effects in air. Currently, he is also a scientist in the nano-photonic thrust at the Center for Integrated Nanotechnologies.

Mark A. Rodriguez has a Ph.D. in Ceramic Engineering from Alfred University ('92) and has been employed at Sandia National Laboratories for 20 years performing X-ray Diffraction in the Materials Characterization and Performance Department.

Michael Brumbach received his Ph.D. in Analytical Chemistry from the University of Arizona in 2007. He then did his post-doctoral research at Sandia National Laboratories on electrochemical capacitors before joining the staff in the Materials Characterization Department in 2009.

Bonnie McKenzie is a scanning electron microscopist at Sandia National Laboratories.

Julia Craven-Jones is an optical engineer at Sandia National Laboratories. She obtained her Ph.D. in optical sciences from the University of Arizona in 2011.